PCCP

The application of theoretical models of complex shape to the fitting of experimental spectra having closely overlapping bands

Trevor R. Griffiths,*[a] Dmitry A. Nerukh*[a]† and Sergey A. Eremenko[b]

[a] *School of Chemistry, University of Leeds, Leeds, UK LS2 9JT*
[b] *Inorganic Chemistry Department, Kharkov State University, Svobody Sq. 4, Kharkov-77, 310077, Ukraine*

Received 30th March 1999, Accepted 19th May 1999

The problem of the uniqueness of parameters obtained during fitting of experimental spectra containing closely overlapping bands has been evaluated, since conventional methods of fitting do not produce reliable results. It is here shown that, despite the difficulties inherent in both the formal mathematical problem and its numerical solutions, typical and representative spectra can be resolved unambiguously within a reasonably chosen theoretical model. Reliable values of the parameters of the model, including parameters of band shape, can also be obtained. A random search method of global minimisation of a function with a significant number of arguments is derived. A program and algorithm to implement this method for spectra decomposition have been developed. The program allows the microdynamics of liquids to be obtained directly upon performing numerical Fourier transformations on a model (theoretical) time correlation function together with using model spectra obtained thereby in each fitting step. A model spectrum for any desired accuracy and frequency range can hence be generated without the unavoidable errors inherent in conventional methods. The apparatus function of the spectrophotometer is also now readily incorporated. Using the algorithm, the parameters of the microdynamics of acetonitrile molecules are obtainable for the first time upon decomposition of its ν_2 Raman vibration, and a value of 0.069 was obtained for the dimensionless modulation speed in liquid acetonitrile. This method has also enabled for the first time the detection of molecules in the second solvation shell around Li^+ in acetonitrile, from within its Raman spectrum.

When experimental spectra are resolved into separate bands the quality of the fit and information available from the parameters obtained have often not been (fully) explored. Generally, in-house and commercial software use standard least squares methods and only traditional methods of non-linear local minimisation are exploited. If the minimisation is repeated, with different initial values of the various parameters, substantially similar results should be obtained. Unless tests for the uniqueness of parameters are performed the parameters of complicated models, consisting of many bands of complex shape, may be used uncritically in the interpretation of experimental spectra.

The problem of fitting experimental data to theory is not trivial, even for the simplest band shapes. The real problem, in studying "complex" bands, is to obtain certain characteristics of their shape as well as their positions, heights and widths. Knowledge of the shape of each band is frequently required for the model spectrum to be relevant to the experimental one. In addition, obtaining band shapes is, in many cases, the main purpose of the investigation as, for example, for the investigation of dynamic properties. This problem of band shape is usually avoided by using one that is as simple as possible.[1] Generally, Lorentz and Gauss shapes are tested first and the one that fits best taken as the "true" shape. This approach does result in reliable parameters, but obviously limits the extraction of the dynamic properties contained in the experimental data.

The properties of the minimising function play a key role. From general considerations, and based on numerous calculations, we found that the source of the band shape problem is the weak dependence of the optimising function upon the fitted parameters, because a large number of fitting parameters is involved. Also, as well as function non-linearity, there is a strong dependence of one parameter upon another. We shall here show that the minimising function also has several local minima, and that this makes local minimisation methods unworkable.

Besides the technical, purely numerical problems of finding the minimum of the sum of squares of deviations (**SSD**), there are difficulties in interpreting the parameters obtained. The global minimum does not necessarily give the most reasonable parameters: if, for example, we have a set of several local minima, close in **SSD**, the values of the parameters covering all these minima should be considered equally true. This is tightly connected to the problem of choosing a proper theoretical model for fitting. If the model is overestimated, *i.e.*, too detailed, the appearance of such local minima and uncertainties in the values of the parameters are highly probable.

This study describes, and illustrates progressively through examples, a new optimisation method that elucidates complicated profiles of spectra, and the principles involved. Particular attention is given to extracting the parameters of microscopic dynamics from vibrational spectra because this is directly concerned with the problem of obtaining line shapes.

Problem description

The basic problem is to calculate the values of the parameters of the chosen model, not to elucidate the model itself, nor determine the number of bands and the expressions for their shape from the experimental spectra. We use the word "model" to mean the theoretical description of the number of bands and the mathematical expressions of their shape. The number and expressions for these bands have first to be

† On leave from Organic Chemistry Department, Kharkov State University, Svobody Sq. 4, Kharkov-77, 310077, Ukraine.

chosen, based initially on external information such as gas phase spectra, theoretical considerations or past experience. Generally the simplest reasonable model is tested first, and then improved (redefined) iteratively until it provides the best possible approximation to the experimental data. The parameters of this model are then adjusted so their individual profiles, when summed, correspond to the measured spectral profile.

Formal theory

Formally, we obtain the best statistical approximation of the experimental data using regression analysis. The experimental value y that depends on the vector of parameters $\boldsymbol{X}$ in the framework of regression analysis is expressed as

$$y(\boldsymbol{X}) = \eta(\boldsymbol{X}) + \varepsilon \tag{1}$$

Since y is considered a random variable, η is an expectation of y having parameters set to $\boldsymbol{X}$ and ε is the random influence.[2]

The properties of ε are key in any fitting procedure. In a least squares approach it is assumed that all the various random influences can be represented by a single influence ε with normal distribution and zero expectation value. Although this is generally the case, there are alternatives in which other properties of ε lead to substantially different fitting results.[3] These will be explored elsewhere while here the least squares approach only will be discussed.

It is hence assumed that ε is non-correlated at each measured point.[2] Thus, strictly speaking, the least squares method is not applicable if the theoretical model is too primitive and thus partly included in the random influence second term of eqn. (1). In practice, however, it is difficult to avoid any correlation in ε, and plots of the residuals, $\varepsilon = y(\boldsymbol{X}) - \eta(\boldsymbol{X})$, often indicate some trends, especially in the wings of spectral bands in the case of spectra decomposition.

When solving the least squares problem, therefore, for spectra decomposition, we minimise the function

$$Q(\boldsymbol{X}) = \sum [I^{\mathrm{e}}(\nu_i) - I^{\mathrm{t}}(\nu_i, \boldsymbol{X})]^2, \tag{2}$$

where I^{e} is the experimental spectral intensity at frequency ν_i and I^{t} is the value of the model function calculated in ν_i point. The summation is performed through all experimental points. I^{t} however can be expressed in a variety of ways and its properties are essential only for finding the minima of the function Q. If, for example, Newton type methods of minimisation are used, Q (and consequently I^{t}) can be differentiated with respect to $\boldsymbol{X}$, necessary for calculating the gradients of Q. The least squares method does not imply any constraint on the function I^{t}, provided the statistical features of ε are retained. This allows us to construct such non-trivial models as the calculation of I^{t} through the Fourier transformation of the time correlation function or to fit several spectra simultaneously.

The model spectral function is commonly represented as

$$I^{\mathrm{t}} = B + \sum_i I_i^{\mathrm{b}} \tag{3}$$

where B is the base line and I^{b} represents bands of previously chosen shape. The base line is generally a polynomial function of the order 1 to 3, weakly dependent on frequency, and often contains the wings of neighbouring bands, and contributions from, for example, luminescence in Raman bands.

In many practical cases eqn. (3) corresponds to a somewhat idealised model. When the number of bands is large and many overlap extensively it is best to use the infinite summation in eqn. (3). This now produces a more complex model of essentially one spectral outline, avoiding the use of a large number of simple shape bands. However, because of the lack of proper theoretical models (or for the sake of simplicity and in order to solve the problem), a simplified assumption of a finite sum in eqn. (3) can be used.[4]

The common form of the constituent bands I^{b} can be written as

$$I^{\mathrm{b}}(\nu) = S_0\, f(\nu - \nu_{\max}, \sigma, \boldsymbol{b}) \tag{4}$$

where f is real, even, normalised to the integral [or $f(0)$], and can be a symmetrical or unsymmetrical function of the frequency ν. In this context S_0 is characteristic of the height of the band in the summation in eqn. (3), and $\nu_{\max}$ is the position of its maximum, σ the characteristic of the band width, and $\boldsymbol{b}$ the set of parameters characterising the band shape. The first three parameters are always present in any expression of band shape, while the remainder are often omitted, and the shape of the band is defined by a particular form of the expression as in, for example, the following Lorentz and Gauss functions (symbols as above):

$$L(\nu, \sigma_{\mathrm{L}}, \nu_{\max}) = \frac{1}{\pi} \frac{\sigma_{\mathrm{L}}/2}{(\nu - \nu_{\max})^2 + (\sigma_{\mathrm{L}}/2)^2}; \tag{5}$$

$$G(\nu, \sigma_{\mathrm{G}}, \nu_{\max}) = \frac{1}{\sqrt{2\pi}\,\sigma_{\mathrm{G}}} \exp\left[-\frac{1}{2}\left(\frac{\nu - \nu_{\max}}{\sigma_{\mathrm{G}}}\right)^2\right]. \tag{6}$$

From the fitting point of view, $\boldsymbol{b}$ is more difficult to obtain because its influence on I^{t} is the least of all other parameters but even so $\boldsymbol{b}$ can be extracted from experimental spectra.

Non-trivial applications

Non-trivial applications of the formal theory to the spectral resolution problem include the extraction of dynamic properties from the band shape. The time correlation function, $C(t)$, from common expressions of stochastic processes analysis, when obtained as a Fourier transformation of the spectral function given in eqn. (4), may be written as

$$C(t) = \frac{1}{2\pi} \int_{-\infty}^{\infty} f(\nu) \mathrm{e}^{-\mathrm{i}\nu t}\, \mathrm{d}\nu. \tag{7}$$

Moreover, the band width parameter, σ, represents in time space the integral property of the correlation function, the correlation (relaxation) time, τ, *viz.*,

$$\tau = \int_0^{\infty} C(t)\, \mathrm{d}t. \tag{8}$$

Thus for a Lorentz curve we have

$$C_{\mathrm{L}}(t) = \frac{1}{2\pi} \exp\left(-\mathrm{i}\nu_{\max} t - \frac{\sigma_{\mathrm{L}}}{2} |t|\right). \tag{9}$$

Upon normalising, and omitting the purely oscillating part and considering positive time, we have

$$C'_{\mathrm{L}}(t) = \frac{C_{\mathrm{L}}(t)}{C_{\mathrm{L}}(0)} = \exp\left(-\frac{\sigma_{\mathrm{L}}}{2} t\right); \quad \tau_{\mathrm{L}} = \frac{\sigma_{\mathrm{L}}}{2}. \tag{10}$$

Any information concerning the detailed behaviour of the correlation function is thus contained in the parameters of spectral band shape $\boldsymbol{b}$. If we consider the Voigt function, an integral convolution of the Lorentz and Gauss functions, we have

$$I^{\mathrm{b}}(\nu) = S_0 \int_{-\infty}^{\infty} L(\nu - \mu, \sigma_{\mathrm{L}}, \nu_{\max}) G(\mu, \sigma_{\mathrm{G}}, \nu_{\max})\, \mathrm{d}\mu \tag{11}$$

and its Fourier transformation after similar evaluations has the form

$$C(t) = \exp\left(-\frac{\sigma_{\mathrm{L}}}{2} t - \frac{\sigma_{\mathrm{G}}^2}{2} t^2\right) \tag{12}$$

Thus all the information about the dynamic features of this function is enclosed in the ratio of corresponding widths β_{V}, *viz.*, $\sigma_{\mathrm{G}}/\sigma_{\mathrm{L}}$. To extract dynamic information from the experimental spectrum we have, therefore, to obtain information concerning the line shape of the spectrum.

Non-trivial models of the spectrum

Obtaining molecular dynamics directly

Molecular dynamics can be obtained directly from the fitting procedure. Since physical theories of microscopic dynamics operate in time space, their correlation functions often do not have an analytical representation in frequency space (or these expressions are particularly complicated). One such is the Kubo function,[5] which is widely used in the description of vibrational relaxation and in Raman spectra of isotropic scattering, and can be expressed as:

$$f_{\mathrm{vib}}(t) = \exp\left\{-M_2\,\tau_\Delta^2\left[\exp\left(-\frac{t}{\tau_\Delta}\right) - 1 + \frac{t}{\tau_\Delta}\right]\right\}, \qquad (13)$$

where M_2 is the second spectral moment of the band, and τ_Δ is the relaxation time of the environment fluctuations.

The Fourier transformation of a Voigt function is relatively simple, eqn. (12), even though the function itself, eqn. (11), does not have an analytical representation that makes its calculation any more time consuming than, say, the product of Lorentz and Gauss functions. Conversely, the numerical Fourier transformation of the experimental data always suffers from unavoidable sources of error. These include the cut-off of the spectra on the ends of the frequency range. This leads to non-physical oscillations in time space. There are also a finite number of data points, and the influence of the apparatus function on the "true" spectrum.

New route to time characteristics and apparatus function

We now propose another approach for fitting spectra to obtain time characteristics that avoids all the above restrictions. This involves performing numerical Fourier transformations on the model (theoretical) time correlation function and using model spectra obtained by this procedure in each fitting step. The advantage is the generation of a model spectrum to any desired accuracy and over any required frequency range. The apparatus function of the spectrophotometer is readily incorporated in this approach because the measured spectra are the integral convolution of the "true" spectra and the apparatus function, that is, a simple product of the appropriate correlation functions.

The calculation of the Fourier transformation in each step of the fitting process is not time consuming, since a fast Fourier transformation algorithm makes the calculation time comparable with, say, the calculation of a Voigt function by series.

Fitting several spectra simultaneously

Another substantial improvement to spectra decomposition is "multi-spectra" fitting. Here the calculation of the squares of deviations can be performed by summation over several spectra using

$$Q(\boldsymbol{X}) = \sum_{j=1}^{n}\sum_{i=1}^{k}\left[I_j^{\mathrm{e}}(\nu_i) - I_j^{\mathrm{t}}(\nu_i, \boldsymbol{X})\right]^2, \qquad (14)$$

where n is the number of spectra undergoing decomposition and k the number of data points in each spectrum. This is useful when a series of spectra have to be fitted and we can assume that the several common parameters all have the same value in all spectra. For a series of spectra of a particular system at different temperatures we can assume that, for example, only the heights of the bands are subject to change, while all other parameters remain the same. This reduces the number of fitting parameters and provides necessary links between different spectra. The approach is particularly advantageous for isotropic and anisotropic Raman scattering spectra. Such spectra are very similar in origin and differences between them provide subtle details concerning the structure and dynamics of the species under investigation.

Profiles of minimising functions

Profiles of SSD and meaning of corresponding parameters

The problem of finding a reliable or correct set of parameters during fitting is twofold. First, the minimum (or minima) of the SSD needs to be found and, second, the behaviour of the SSD around the minimum must be analysed since it gives an estimation of the confidence interval of the parameters obtained. Regarding the latter, there are no universal methods for describing the multi-parameter function profiles, especially when they are non-linear and multi-modal. Moreover, the existence of the multitude of local minima makes the standard estimation of the confidence intervals of fitting parameters unworkable because all such methods are for analysing local minima. However, using test calculations, and general considerations concerning the complexity of the theoretical model under fitting, several typical cases can be distinguished.

Fig. 1 shows three model cases for the dependence of the SSD with respect to one optimising parameter. Case (a) is preferred as the function has a single, well-pronounced minimum which is lower than the experimental SSD (Q^{e}). Unfortunately this idealised situation is never reached in practice. Cases (b) and (c) are more realistic, representing simple and complex theoretical functions, respectively. If too simple a model is defined, the SSD will have a single minimum, but well away from the experimental SSD. SSD values of more complex models approach the experimental result but tend to have multiple local minima and a wider "spread" (*d*).

The value of this spread will essentially define the confidence interval of the parameter. In practice, we find several local minima and estimate the confidence interval as the interval between minima with equal SSD. The local minima problem may be complicated if the function has very shallow minima, indicating weak dependence on the parameter, or if it exhibits both several local minima and a weak dependence on the parameters. The number of significant digits of the parameter depends upon its confidence interval in a non-simple way.[6] In this study we do not analyse confidence intervals of the parameters in detail but here give as many digits of the parameters as necessary. The number of digits in this case does not reflect the error in the parameter and is not connected to the experimental uncertainties in its determination. Hence we do not present confidence intervals in the tables but give as many digits as needed to show the changes in the parameter in different calculations.

Existence of a unique minimum

In the numerical minimisation of the multi-parameter function it is difficult to determine whether it is or is not uni-modal (having a single minimum). The problem is more difficult if we have more than around ten parameters or features that complicate the finding of local minima, *e.g.*, a strong dependence between several parameters. Here local minimisation methods terminate at different points and it is not possible to determine whether they have reached a local minimum or the method has failed. Although there is no unambiguous or correct recipe for analysing the object function, based on a large number of trial calculations, some predictions about its behaviour can be made.

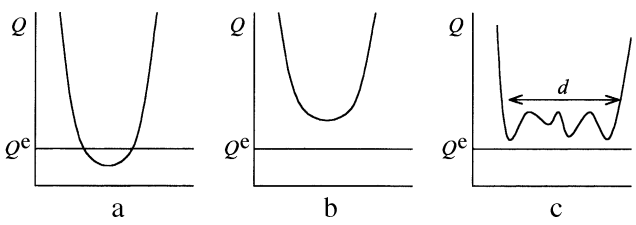

Fig. 1 Typical cases of the behaviour of SSD (Q) with respect to an optimising parameter. Q^{e} is the experimental SSD.

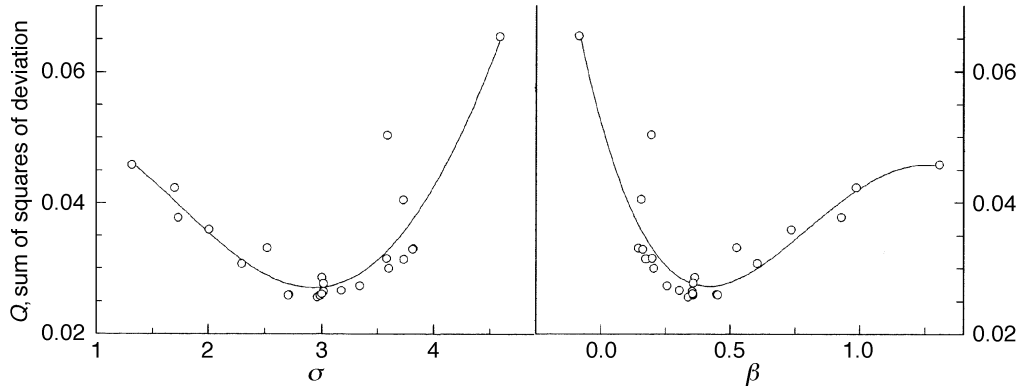

Fig. 2 Dependence of sum of squares of deviations upon two adjustable parameters: $\sigma = \sigma_L$, band width; $\beta = \beta_V$, ratio of Lorentz and Gauss band components. Circles are values obtained from several fittings of the acetonitrile Raman spectrum using the Simplex method[7,24] from different initial parameter values. These show that while the Simplex method does not give the desired solution, the profile of the minimising function has a single minimum.

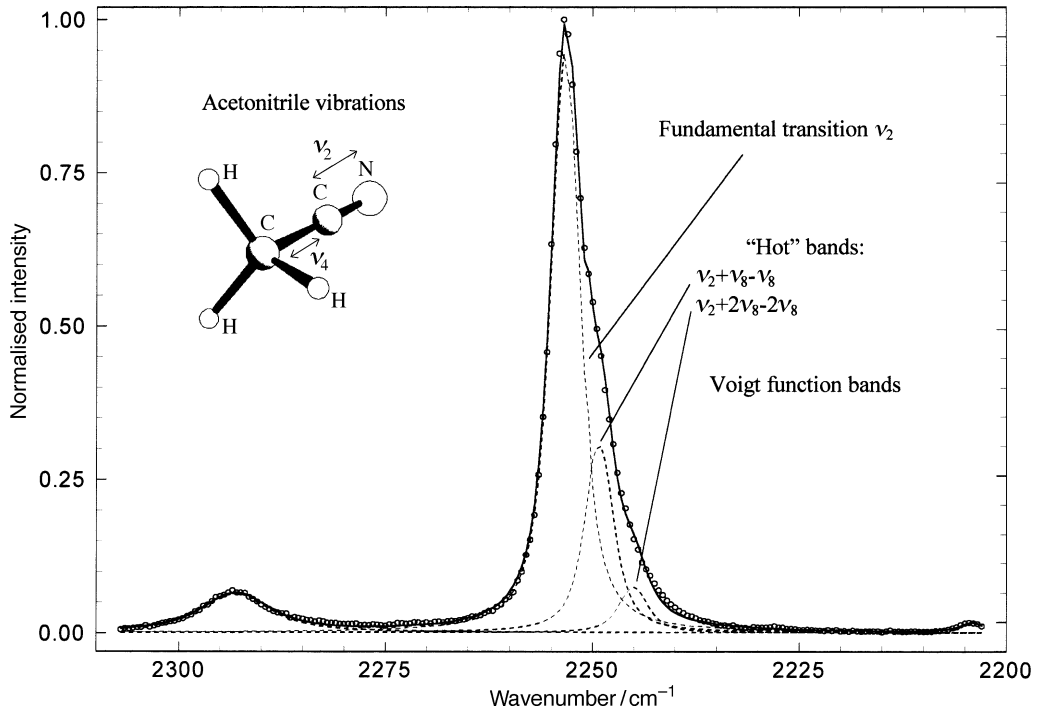

Fig. 3 Isotropic Raman scattering of acetonitrile at 25 °C and its decomposition into Voigt function bands to obtain vibrational relaxation parameters. Significant overlapping of the bands around 2250 cm^{-1} hinders the determination of their shape.

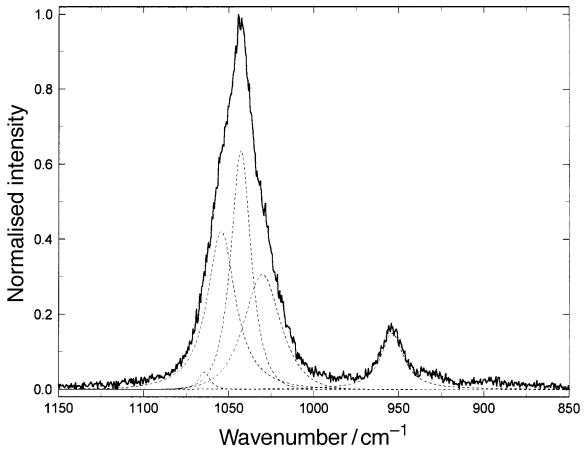

Fig. 4 Isotropic scattering spectrum of dimethyl sulfoxide with its resolution using Lorentz band shapes: an example of a highly overlapping set of bands for which obtaining a reliable or correct set of parameters, despite the simple shape of each band, is complicated.

If strong correlations between several parameters are present[2] (for example, between the band width of Gaussian and Lorentzian components) the possibility of multiple local minima all having very similar minimising functions is high. This situation can be easily recognised in spectra decomposition when, for example, some closely overlapping bands compensate each other and these lead to small change in the squares of deviation Q, within experimental error.

Despite the above caveats, if we have a situation similar to that shown in Fig. 2, it can be confidently concluded that the function has one unique minimum. In this diagram the resulting SSDs from many fittings of the experimental spectrum are shown, starting from different initial values of the parameters. This surface has a global minimum since all these points lie on the surface of the minimising function.

Sources of peculiarities

The results of comparing various ways of spectra fitting with various models has shown that there are two main sources for

the appearance of multiple minima in the function of the squares of deviations Q. First, if a model theoretical spectrum is not smooth, but has some non-physical step character, this can lead to similar apparent noise in the minimising function that is large enough to be considered as local minima by the minimisation algorithm. This situation was found in the fitting of the isotropic spectra of acetonitrile (Fig. 3) using Voigt band shapes, eqn. (11), calculated by series. Second, even if our model function is completely smooth, if the bands overlap considerably this can produce several adjacent minima in the object function. This arises from the contribution of a few bands and this in turn can be compensated by contributions from other bands. This type of compensation can be seen in the Raman spectra of dimethyl sulfoxide (Fig. 4). The contribution of the closely sited bands around 1050 cm^{-1} can be represented, with less accuracy, by a single band. Therefore, the heights of these two bands can be allowed to vary provided that their sum remains approximately constant.

Method of fitting

Local optimisation methods

The success of our new fitting method and the results obtained depend on the features outlined earlier. However, the most valuable component is the algorithm used for the minimisation of the sum of deviations. Since the theory of local minimisation is now well developed,[7] various methods of local minimisation are a natural choice for the spectra decomposition problem.

There are two main categories of these algorithms, gradient and non-gradient. Although algorithms of the first category are generally faster they require the calculation of derivatives of the minimising function with respect to its parameters. The effectiveness of these algorithms depends largely upon the accuracy of calculation of the derivatives. This is not a problem if the derivatives can be calculated analytically. Unfortunately this is frequently difficult to perform, or impossible in principle. For example, the function in eqn. (13) does not have analytical derivatives with respect to its parameters.

Among non-gradient methods the flexible Simplex method is stable and effective for problems with a large number of parameters,[7] and hence was our choice for fitting calculations. However we found that this method does not work for spectra decomposition, and whether this is because it finds only local minima or cannot find any minima is not apparent (but see later). The difficulties and problems arising with gradient and non-gradient algorithms can be overcome if a method for global minimisation is employed. This method guarantees finding the minimum, even if it is the only minimum of the function.

The algorithm has also to work when a large number of parameters is involved. Within the diversity of global search algorithms[8] the random search class of algorithms proved suitable for functions of this type. Such algorithms are attractive as they allow substantial modifications and they are flexible and adaptable for a variety of problems.

Random search algorithm

The general description of the algorithm[9] is as follows:

1. Generate N times random multidimensional points x_1^0, …, x_N^0 with distribution $P_0(dx)$ and assume $s = 0$, *i.e.*, any number of variables can be fitted.
2. From the points x_i^s choose l points x_{1*}^s, …, x_{l*}^s with the least values of the object function.
3. Based on some rule (described later) define numbers n_i ($i = 1, \ldots, l$) such that $\sum_{i=1}^{l} n_i = N$.
4. For all $i = 1, \ldots, l$ generate n_i times the distribution change $P_s(x_{i*}^s, dx)$, obtaining points $x_1^{s+1}, \ldots, x_N^{s+1}$.
5. Go to step 2 changing s to $s + 1$.

In our version of this random search algorithm N was 20, …, 100, and n_i ranged from 1 to 10. Several rules in step 3 were investigated, including the dependence of n_i on the value of the object function in the point x_{i*}, but as this did not affect the efficiency of the algorithm, we chose the simplest case, when all n_i are equal.

The key feature of this algorithm is the character of the distribution change P_s. To provide a reasonable convergence of the search the "widths" of the distributions must not increase with the iteration process. We thus used normal distributions centred on x_{i*}^s and having dispersions d for P_s, and P_0 was found not to influence the properties of the algorithm. P_0 is centred on the initial values of the parameters, which can be chosen ambiguously, and its dispersion may have any reasonable value (*e.g.*, initially equal to 50% of the parameters) as it is quickly altered to the optimal value during the next few steps. More important is d for P_s, which defines how "close" the points on each successive step are generated to the points in the previous step. The behaviour of d from step to step defines both the speed of the algorithm and its global character. If it shrinks rapidly, the points cover too limited a range of parameter values, and we risk not finding the global minimum. If d decreases slowly, the speed of convergence slows, and the calculation is not completed in reasonable time.

To obtain d we tested two approaches for its calculation. The first used the statistical characteristics of the distribution of x_{i*}, the behaviour of the object function on the current step. In the simplest case d is set equal to the dispersion of the distribution of x_{i*}. In the second approach, if d decreased when the current step did not produce the "better" point the value of the function in all generated points was thus less than the minimum value of the previous step. Conversely, if a "better" point was found, d increased. Interestingly, the results produced by both these approaches were essentially the same and hence we do not subsequently identify the method used.

Testing the algorithm

We tested our algorithm on the generalised Rastrigin function (Fig. 5), specifically:

$$f = \sum_{i=1}^{n} b_i x_i^2 - \sum_{i=1}^{n} \cos(18x_i) \qquad (15)$$

The numbers of parameters employed were n up to 20, b_i equal to 0.001 for $i = 6$ and 0.0001 for $i = 7$ and unity for all other i. In all cases the global minimum was found, and the calculation time depended on the number of parameters and set of coefficients b_i used. Although this function is quite complex for finding the global minimum our algorithm produced the correct solution in all cases, despite a significant number of parameters, the very different scales of dependence on different parameters, and the large number of local minima in the vicinity of the global minimum.

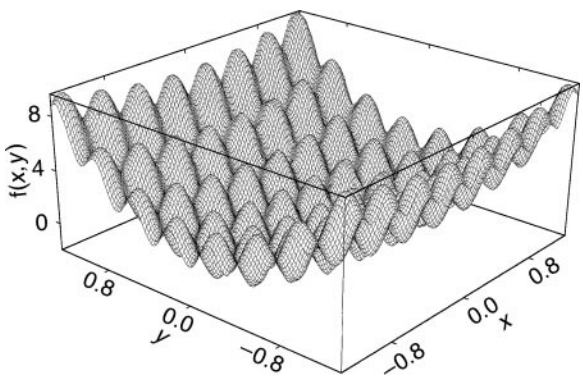

Fig. 5 View of function $f = x^2 + 4y^2 - \cos(18x) - \cos(18y)$ showing the multitude of local minima. This function was used as a test for evaluating the efficiency of our global optimisation algorithm.

Implementation of the algorithm

A programming problem arises when using least squares for spectra decomposition because the procedure requires the examination of many descriptions of theoretical spectra. There are no difficulties in coding for this if, for example, only the number of bands is altered, but this is inconvenient when using non-trivial shapes for different bands in a spectrum. Our approach for defining the theoretical model overcomes this.

We describe the theoretical spectrum, fixing its parameters and all other necessary information for governing the optimisation process, in a language similar to natural mathematical language. The model is thus easily varied, including both the number of bands and their shape, and we can also define the whole spectrum not just in terms of bands but through, for example, Fourier transformation of the correlation function, as described earlier. A typical example of the description of model spectra is given in the supplementary data.‡ The program for spectral data handling and spectra decomposition uses object oriented programming and runs under OS/2, Win32 and UNIX and is coded in standard C++ and hence can be easily transferred to other operational systems.

Results and discussion

The results presented here aim to show the uniqueness of the parameters obtained from fitting various theoretical models to various experimental spectra with different levels of complexity from the fitting point of view. It is important to stress that the values of the parameters and, consequently, their physical meaning depend crucially on the theoretical model chosen. Analysing the numerical values of the parameters and comparing them with literature values allows us to determine the quality and appropriateness of the theoretical model used for fitting each particular spectrum. Naturally, drawing conclusions from a comparison of the values of parameters without careful analysis of the underlying theoretical model must be avoided. We outline the meaning of the parameters presented here, but a detailed discussion is not appropriate now. The conclusions presented here, however, do provide the necessary background for subsequent analysis of the physical meaning of the parameters since we cannot interpret a value without being sure of its uniqueness.

‡ Available as supplementary material (**SUP 57565**, 4 pp.) deposited with the British Library. Details are available from the Editorial Office. For direct electronic acess see http://www.rsc.org/suppdata/cp/1999/3199.

Resolving several highly overlapping bands of simple shape

Our algorithm was first tested using a relatively simple decomposition problem. Lorentz and Gauss band shapes were used to resolve experimental spectra consisting of four to six considerably overlapping bands. Three examples are now discussed.

Fullerene spectra. A typical, and topical, example is the luminescence spectrum of a thin film of fullerene. We had earlier[10] examined the structures arising from varying the method of preparation and the resulting thickness of these films. This was in part evident from variations in their emission spectra in the visible region, of which Fig. 6 is a typical example. Such spectra theoretically consist of Gaussian-shaped bands and when attempting to fit the profile for the apparent minimum number of bands, using a standard least squares fitting program (PeakFit 4, Jandel Scientific), the band parameters were not independent of the initial estimates. Using the universal procedure described here a unique fit was obtained.

The results of the decomposition are given in Table 1 and it can be seen that, although a range of different initial estimates was employed, the final parameters obtained were identical within experimental error. It is important to stress that although the choice of Gaussian bands was dictated by theory,[10] the theory is not confirmed by this resolution, but the fit is unique to the observed profile.

Acetonitrile spectra. Fig. 3 shows the isotropic Raman scattering of the ν_2 vibration of acetonitrile. We have previously reported[11,12] preliminary structural and dynamic characteristics of liquid acetonitrile, from an initial resolution of this spectrum. We now use the numerical approach to obtain more detailed information on these characteristics and present a more general form that can be used for essentially all types of spectra.

The model consists of four Lorentzian bands and the problem was simplified by introducing a relationship between the parameters, namely that the widths and heights of "hot" bands were expressed through the width and height of the fundamental transition band. The shift of the origins of these bands was also defined by a single parameter. However, using these simplifications neither the Simplex nor the Levenburg–Marquardt methods, implemented in PeakFit, gave a unique solution: the derived parameters depended upon the initial estimates. Our random search algorithm, however, was particularly successful and produced identical results after several fitting runs starting from a range of initial values. Table 1 con-

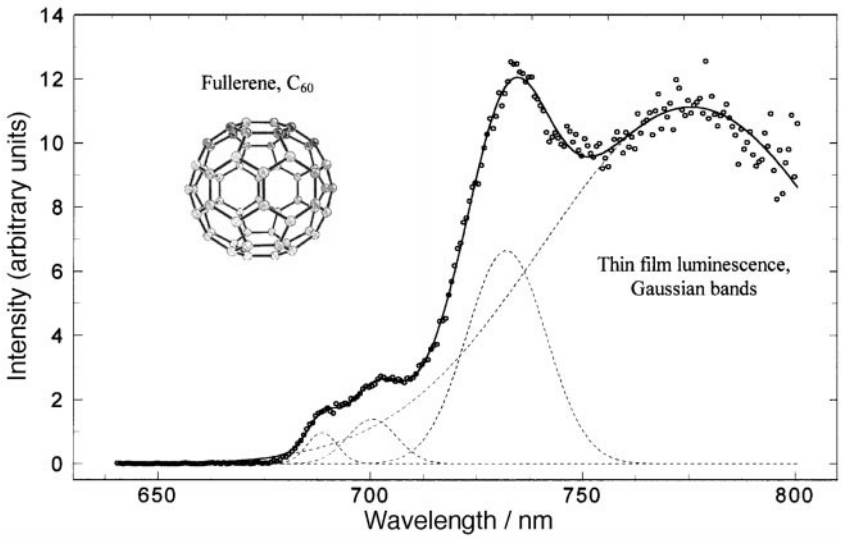

Fig. 6 Luminescence spectrum of a thin film of fullerene C_{60} and its resolution into Gaussian bands.

Table 1 Decomposition of spectra consisting of closely overlapping bands of simplest shape[a]

(a) Luminescence spectrum of the fullerene C_{60} thin film, four Gaussian bands fit

	Band 1			Band 2			
N	S_0 (arbitrary units)	ν_{max}/cm^{-1}	σ_G	S_0 (arbitrary units)	ν_{max}/cm^{-1}	σ_G	D
1	1.55600	732.004	9.34283	0.201232	700.450	5.75883	0.309875
2	1.55600	732.004	9.34283	0.201231	700.450	5.75882	0.309875
3	1.55601	732.004	9.34283	0.201233	700.450	5.75887	0.309875
4	1.55601	732.004	9.34283	0.201232	700.450	5.75883	0.309875

(b) Isotropic Raman scattering of dimethyl sulfoxide, five Lorentzian bands fit

1	21.6337	1042.8224	16.6736	6.6518	1028.4732	18.2274	7.8133×10^{-2}
2	21.6149	1042.8225	16.6652	6.6615	1028.4793	18.2398	7.8133×10^{-2}

(c) ν_2 vibrational spectrum of isotropic Raman scattering of acetonitrile, four Lorentzian bands fit

	Band 1				
N	S_0 (arbitrary units)	ν_{max}/cm^{-1}	σ_L	Δ_{hot}	D
1	5.503522	2253.431	3.718804	3.491379	5.7172×10^{-5}
2	5.503525	2253.431	3.718807	3.491377	5.7172×10^{-5}
3	5.503521	2253.431	3.718804	3.491377	5.7172×10^{-5}
4	5.503520	2253.431	3.718803	3.491380	5.7172×10^{-5}

[a] N is the computation number; S_0 (arb. units), ν_{max} (cm^{-1}) and $\sigma_{G,L}$ (cm^{-1}) are the height, maximum position and width, respectively; Δ_{hot} (cm^{-1}) is the shift in positions of "hot" bands; and D is the approximation dispersion. Several representative parameters are given to illustrate typical cases in the uncertainties of their determination. These uncertainties originate from the fitting procedure and do not have any direct connection with the experimental error of the measured spectra. The number of digits shown is more than normally required to represent the experimental error, but here shows the excellent quality of the fitting parameter.

tains a selection from many of the results obtained for one of the four resolved bands.

There are several reported attempts to fit the vibrational spectra of liquid acetonitrile,[13–16] all very different in their manner of treating the number of bands and their shape. Consistency within the model is most important for comparing results. For example, if the positions and widths of the "hot" bands are considered as independent parameters this changes the width of the fundamental ν_2 band from 3.72 (in our model) to 4.12 cm^{-1}. Both values are "true" from the fitting point of view, because they are unique in the framework of the corresponding theoretical model. An analysis of the features of these published models, taking into account where possible results from other experiments and theoretical treatments, is required for choosing the "correct" value from the physical point of view. A review of such models and their analyses will be published elsewhere.

Dimethyl sulfoxide spectra. A more complex model was required for the decomposition of the Raman spectrum of dimethyl sulfoxide (DMSO), Fig. 4, in terms of the increased number of parameters used. Again we obtained a unique solution, Table 1. This spectrum was represented by five bands and these give, together with the base line, 17 adjustable parameters. Interestingly, this profile contains three independent highly overlapping bands of comparable height. This situation could lead to significant uncertainties in results that cannot be resolved by standard methods.

However, the existence of several local minima with approximately equal SSD values in the vicinity of the global one is highly probable. In this case the parameters obtained from any of these minima may be considered true, the choice depending upon external information, or the whole model should be reformulated in order to exclude these minima.

The set of bands in this model corresponds to different types of DMSO associates and our results reveal more statistically justified bands than in the other published data.[17,18]

Parameters of band shape

Three different band models having adjustable shape parameters and the three basically different fitting situations they represent are now examined. In all cases standard algorithms do not work, and the random search method was thus employed.

Over-estimated model resulting in several local minima. The spectrum of dimethyl sulfoxide in Fig. 4 contains bands that are based on the product of Lorentz and Gauss curves:[19]

$$I(\nu) = \frac{S_0}{1 + 2^{1-\beta_S}\left(\frac{\nu_{max} - \nu}{\sigma_S}\right)^2} \exp\left[-\beta_S \ln(2)\left(\frac{\nu_{max} - \nu}{\sigma_S}\right)^2\right] \quad (16)$$

The advantage of this type of model is that the speed of calculation is rapid. It is also expressed analytically, so that it excludes any source of calculation errors leading to roughness in the squares of deviation and, consequently, local minima of this type, as defined earlier. Numerous calculations with various modifications of the algorithm have shown that it is likely that there are several, but not many, minima that are the consequence of considerable overlapping of the constituent bands. These solutions are reported in Table 2.

Naturally, the "true" solution should be chosen and this is the one minimum value of the approximation dispersion. This example shows that when the theoretical model is overestimated, local minima appear even if band shapes are particularly simple. In this case conclusions based on subtle details of the results of spectra decomposition must be treated with care: any of these minima can be considered as true and the corresponding parameters have wide confidence intervals that cover all these minima.

Voigt band shapes. Tests showed that Lorentz and Gauss

Table 2 Decomposition of spectrum of isotropic Raman scattering of dimethyl sulfoxide, using the product of Lorentz and Gauss functions [eqn. (15)] used as band shape[a]

N	S_0 (arbitrary units)	ν_{max}/cm^{-1}	σ_S/cm^{-1}	β_S	D
1	0.420	1054.384	13.860	0.0795	5.7761×10^{-2}
2	0.415	1054.431	13.640	0.0835	5.7799×10^{-2}
3	0.392	1054.306	13.414	0.2780	5.7537×10^{-2}
4	0.396	1054.300	13.491	0.2557	5.7528×10^{-2}

[a] Symbols as in Table 1; σ_S (cm^{-1}) is the width of one of the five bands; and β_S is the band shape parameter (dimensionless). Several representative parameters again shown as in Table 1. Band positions are determined with the highest accuracy, followed by band height and width.

type band shapes are less appropriate than the Voigt function band shape for fitting the acetonitrile spectrum, Fig. 3, especially away from the peak position. However, although the fit is better with this function, the problem of obtaining unique values of the band shape parameters now arises.

A model based on the Voigt band shape was used for the decomposition of this spectrum. This model is rather difficult to employ as a strong dependence between widths exists, eqn. (11), but the consequent change in shape can be partly compensated by a shift of the hot bands. A unique solution is however obtained, Table 3, in the sense that both the approximation dispersion and the parameter values are essentially the same. This example clearly demonstrates that the shape of the bands can be obtained during fitting, even when there is considerable band overlap.

Kubo function. The most interesting model from the physical point of view has bands expressed through a time correlation function,[20] and allows us to obtain microdynamic parameters directly from experimental spectra. The set of bands investigated are again those in the isotropic Raman scattering of acetonitrile, Fig. 3, but the bands are now defined as a Fourier transformation of the Kubo function, eqn. (13). The dependence between τ_Δ and M_2 appeared to be even greater than in the case of the Voigt function. This slowed the speed of the calculations, but a solution was obtained, Table 3.

Comparison of band models. The slight difference in shape parameters in the latter two cases is due to a small influence of these parameters on the sum of deviations.[6] We obtained excellent shape parameters even though the fitting was started with very different initial estimates, sometimes by several orders of magnitude.

To our knowledge, this is the first attempt to obtain the parameters of the dynamics of molecules from vibrational spectra having highly overlapping bands. In a previous publication[15] somewhat unjustified assumptions were made in the treatment of neighbouring bands and of band shapes.

We now establish that the latter two models are a significant improvement in the fitting of spectral profiles. The rationale is in the comparison of the approximation dispersions with the dispersion of the experimental errors. The latter was evaluated by assuming a linear "true" spectrum over a narrow range of wavenumbers, from 2350 to 2330 cm^{-1}, Fig. 3. The approximation dispersion could then be calculated and the results were: experimental dispersion, 2.16×10^{-7}; approximation dispersions for the Lorentz model, 5.72×10^{-5}; for the Voigt model, 2.06×10^{-5}; and for the Kubo model, 3.84×10^{-5}. We hence conclude that all these parameters have a good statistical basis, and that there are still opportunities for further improvement of the model. For example, if the accuracy of the experimental spectrum was improved this would allow parameters of an even more complex theoretical model to be obtained, such as parameters of a more complex vibrational correlation function.

Acetonitrile solutions

Fig. 7 shows the resolution of a complex spectral profile, the isotropic spectrum of $LiBF_4$ solution in acetonitrile. For the first time a band has been resolved that can be identified with acetonitrile molecules in the second solvation shell. The theoretical model here is particularly complex: it consists of 12 bands (positions indicated by arrows) that in turn give 22 adjustable parameters. Bands 1 and 7 are weak but are clearly present. The latter corresponds to vibrations of second shell acetonitrile molecules (see below). However, the values of all parameters are unique and the presence of all the bands in the resolution is necessary. Further, the band shape parameter of the fundamental bands 8, 9, 10 and 11 can be obtained: their physicochemical data can be summarised as characteristics of vibrational relaxation of the solvent molecules in solution. This result is particularly interesting because it allows comparison with the dynamics of the molecules in pure acetonitrile (see above) and the results of theoretical and computer modelling.[21]

Table 3 Decomposition of the ν_2 vibrational spectrum of isotropic Raman scattering of acetonitrile[a]

(a) Four Voigt function bands fit [eqn. (11)]

N	S_0 (arbitrary units)	ν_{max}/cm^{-1}	σ_L/cm^{-1}	β_V	D
1	35.087	2253.323	2.836	0.178851	2.0554×10^{-5}
2	34.880	2253.315	2.827	0.174938	2.0510×10^{-5}

(b) Four bands fit expressed through Fourier transformation of Kubo function [eqn. (13)]

N	S_0 (arbitrary units)	ν_{max}/cm^{-1}	M_2 (arbitrary units)	τ_Δ (arbitrary units)	D
1	0.49474	2253.336	498	3085×10^{-3}	3.842264×10^{-5}
2	0.49484	2253.342	521	2950×10^{-3}	3.842264×10^{-5}

[a] Symbols as in Table 1; σ_L is the width of the fundamental band; β_V is the ratio of Lorentzian and Gaussian parts of the band width; and M_2 (arb. units) and τ_Δ (arb. units) are parameters of the Kubo function. Several representative parameters again given as in Tables 1 and 2. Band positions are determined with higher accuracy than band height and width. The band shape parameters β_V and, especially, M_2 and τ_Δ are obtained with lowest accuracy but nevertheless still have satisfactory relative errors: 3–5% for β_V and τ_Δ and ~30% for M_2.

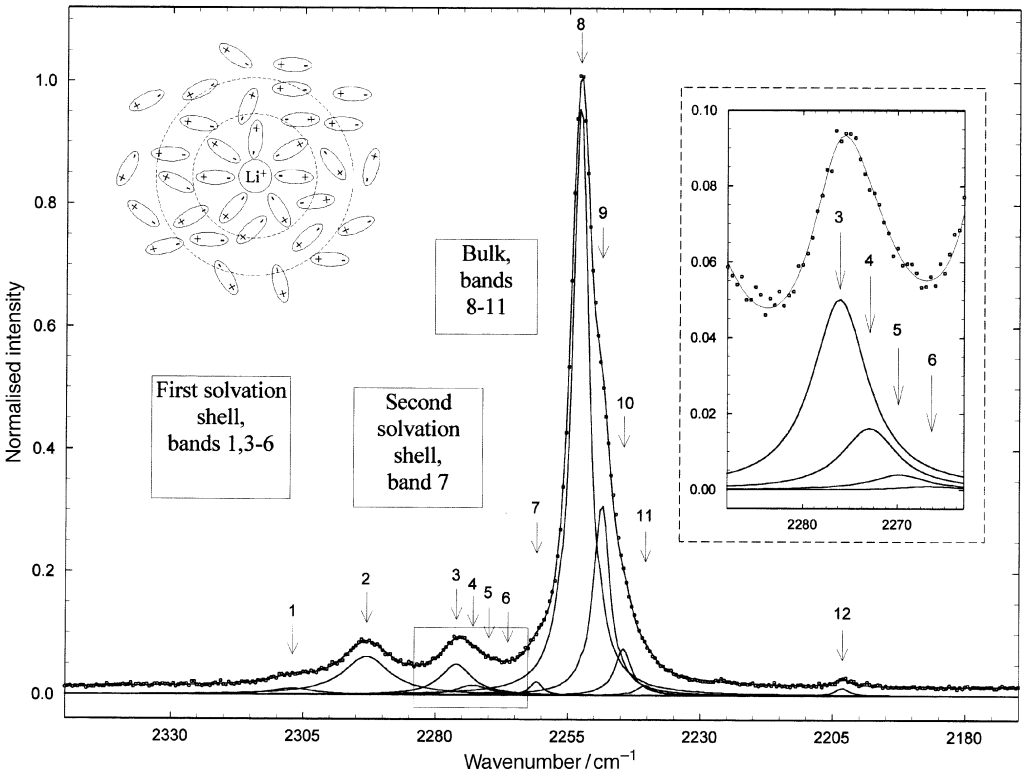

Fig. 7 Isotropic Raman scattering of a solution of $LiBF_4$ in acetonitrile at 25 °C and its decomposition into Voigt function bands using time space representation. Despite the extremely complex theoretical model used to fit this spectrum, the parameters of band 7 and the shape characteristics of bands 8–11 are obtained uniquely.

Obtaining dynamics from experimental spectra. If the instantaneous frequency of the molecular vibration is assumed to consist of the frequency of an isolated molecule ω_0 that fluctuates under the influence of the environment part $\omega_\Delta(t)$, the dynamic feature, the speed of modulation can be characterised by the quantity

$$\sqrt{\langle\omega_\Delta(t)\rangle}\,\tau_\Delta, \qquad (17)$$

where $\langle\omega_\Delta(t)\rangle$ is the mean value of the fluctuations of $\omega_\Delta(t)$ and τ_Δ is its correlation time, provided that its correlation function is assumed to be exponential.[22] The modulation of the vibrations of acetonitrile molecules is known to be fast in the bulk liquid. This is consistent with the Lorentz band shape fitting the experimental spectra well and from the results of Fourier transforms of the experimental spectra using some rather rough assumptions.[13,23] In both studies the exact value of the speed of modulation was not given. Using our algorithm we obtained for the first time the dimensionless speed of modulation in liquid acetonitrile as 0.069. This result is based on the analysis of complicated band shapes, described above, and could not be achieved using traditional methods of spectra decomposition.

Dynamic information can also be carried by parameters other than band shape. The presence of the band itself can serve as a dynamic characteristic. For example, the additional bands identified in electrolyte solutions of acetonitrile compared with pure acetonitrile spectra indicate that the lifetime of the solvent molecules in the first and second solvation shell of the ion is greater than $\sim 10^{-12}$ s, a characteristic time for vibrational spectroscopy. The bands 3–6 are identified with the first solvation shell and are well established,[23] but using our algorithm we found the parameters of the new band 7. This band is here attributed to the response of the solvent molecules in the second solvation shell because it is weaker than those identified with the first solvation shell (bands 3–6), and because it is located between the bulk and primary solvation shell bands.

Experimental

Films of the fullerene C_{60} were prepared by vacuum deposition on NaCl monocrystal. The crystal was then dissolved in water and the 10 nm thick film was floated on to a copper net. The unit cell was measured as 1.420 ± 0.001 nm. Luminescence spectra were recorded at 5 K using excitation lines at 436 and at 546 nm. Acetonitrile was distilled four times, initially twice from P_2O_5, and the third time from K_2CO_3. Dimethyl sulfoxide was purified by fractional crystallisation. Raman spectra were measured using 0.5 cm^{-1} data point intervals on a Ramanor U-1000 spectrometer (Jobin Yvon) with resolution 0.15 cm^{-1} (ref. 24).

Acknowledgements

The authors thank Dr O. N. Kalugin, Kharkov State University, Ukraine, for helpful discussions and Drs V. P. Gnezdilov and A. A. Avdeenko, Kharkov Institute for Low Temperatures, Ukraine, for experimental assistance. DAN thanks the Royal Society and NATO for a Postdoctoral Research Fellowship and the School of Chemistry, University of Leeds, for hospitality during the Fellowship tenure.

References

1 M. Besnard, M. I. Cabaco and J. Yarwood, *Chem. Phys. Lett.*, 1992, **198**, 207.
2 I. Vuchkov, L. Boyadzhieva and E. Solakov, *Applied Linear Regression Analysis*, Financy i statistika, Moscow, 1987.
3 D. S. Konyaev, S. A. Merny and Yu. V. Kholin, New software for studying of equilibrium of complexes formation, *XIV Ukrainian Conference on Inorganic Chemistry*, 1996.
4 O. N. Kalugin, D. A. Nerukh, I. N. Vunnik, E. G. Otlejkina, Yu. N. Surov and N. S. Pivnenko, *J. Chem. Soc., Faraday Trans.*, 1994, **90**, 297.
5 R. Kubo, *J. Phys. Soc. Jpn.*, 1962, **17**, 1100.

6 R. J. Le Roy, *J. Mol. Spectrosc.*, 1998, **191**, 223.
7 D. M. Himmelblau, *Applied Nonlinear Programming*, McGraw-Hill, New York, 1972.
8 A. G. Zhilinskas, *Global Optimisation*: *Axiomatics of Statistical Models*, *Algorithms*, *Applications*, Mokslas, Vilnjus, 1986.
9 A. A. Zhiglyavsky, *Mathematical Theory of Global Random Search*, LGU, Leningrad, 1985.
10 A. A. Avdeenko, V. V. Eremenko, N. I. Gorbenko, P. V. Zinoviev, D. A. Nerukh, A. T. Pugachev, N. B. Silaeva, Yu. A. Tiunov and N. P. Churakova, *Sverkhtverdye Materialy*, 1997, **3**, 54.
11 O. N. Kalugin, D. A. Nerukh, S. A. Eremenko, A. V. Vankevich and A. G. Nerukh, *Zh. Neorg. Khim.*, 1996, **41**, 261.
12 D. A. Nerukh, PhD Thesis, Kharkov, 1996.
13 S. Hashimoto, T. Ohba and S. Ikawa, *Chem. Phys.*, 1989, **138**, 63.
14 A. Sugitani, S. Ikawa and S. Konaka, *Chem. Phys.*, 1990, **142**, 423.
15 K. Tanabe and J. Haraishi, *Spectrochim. Acta*, 1980, **A36**, 665.
16 G. Fini and P. Mirone, *Spectrochim. Acta*, 1976, **A32**, 439.
17 M. I. S. Sastry and S. Singh, *J. Raman Spectrosc.*, 1984, **15**, 80.
18 M. I. S. Sastry and S. Singh, *Can. J. Chem.*, 1985, **63**, 1351.
19 I. M. Strauss and M. C. R. Symons, *J. Chem. Soc., Faraday Trans.*, 1978, **74**, 2146.
20 R. Kubo, in *Fluctuations, Relaxation, and Resonance in Magnetic Systems*, ed. D. Ter Haar, Plenum, New York, 1962, p. 27.
21 M. Maroncelli, *J. Chem. Phys.*, 1991, **94**, 2084.
22 W. G. Rothschild, *J. Chem. Phys.*, 1976, **65**, 455.
23 I. S. Perelygin, A. S. Krauze and I. G. Itkulov, *Chem. Phys.*, 1993, **12**, 404.
24 S. A. Eremenko, O. N. Kalugin and D. A. Nerukh, *Proc. Kharkov. Univ., Chem.*, 1997, **1**, 34.

Paper 9/02569C